

# Inorganic islands on a highly stretchable polyimide substrate

Jeong-Yun Sun<sup>1, 2</sup>, Nanshu Lu<sup>2</sup>, Juil Yoon<sup>3</sup>, Kyu-Hwan Oh<sup>1</sup>,

Zhigang Suo<sup>2</sup>, and Joost J.Vlassak<sup>2 a</sup>

<sup>1</sup>Department of Material Science and Engineering, Seoul National University, Seoul 151-742,  
South Korea.

<sup>2</sup>School of Engineering and Applied Sciences, Harvard University, Cambridge, MA 02138,  
USA.

<sup>3</sup>Department of Mechanical Systems Engineering, Hansung University, Seoul 136-792,  
South Korea.

## Abstract

For a flexible electronic device integrating inorganic materials on a polymer substrate, the polymer can deform substantially, but the inorganic materials usually fracture at small strains. This paper describes an approach to make such a device highly stretchable. A polyimide substrate is first coated with a thin layer of an elastomer, on top of which SiN<sub>x</sub> islands are fabricated. When the substrate is stretched to a large strain, the SiN<sub>x</sub> islands remain intact. Calculations confirm that the elastomer reduces the strain in the SiN<sub>x</sub> islands by orders of magnitude.

**Keywords:** SiN<sub>x</sub> islands, polyimide substrates, fracture, stretchability

<sup>a</sup> email: vlassak@esag.deas.harvard.edu

Flexible electronic devices may experience one-time or repeated large deformation during manufacture or in service.<sup>1-6</sup> Such a device often integrates a polymer substrate with diverse inorganic materials, such as semiconductors, metals and ceramics. While the polymer can deform substantially, the inorganic materials usually fracture at strains below ~1%.<sup>7</sup> Consequently, the device is stretchable only when the polymer and the inorganic materials are suitably integrated. Examples include inorganic islands<sup>6-9</sup> and buckled inorganic films<sup>10, 11</sup> on polymer substrates.

This paper focuses on inorganic islands on a polymer substrate. For example, islands of a diamond-like carbon on a substrate of an elastomer (PDMS) remain intact when the substrate is stretched beyond 25%.<sup>7</sup> Some applications may require substrates much stiffer than PDMS. However, SiN<sub>x</sub> islands on a stiffer polyimide (PI) substrate crack and debond when the substrate is stretched by only a few percent.<sup>12, 13</sup> The two examples illustrate a tradeoff between the stiffness of the substrate and the stretchability of the structure.

Here we demonstrate that, when a thin layer of PDMS is sandwiched between the polyimide substrate and the SiN<sub>x</sub> islands, the substrate can be stretched beyond 20% without causing the islands to crack or debond. The PDMS interlayer behaves as a buffer, isolating the islands from most of the strain of the substrate. The resulting SiN<sub>x</sub>/PDMS/PI structure is both stretchable and relatively stiff.

We fabricated two sets of specimens, SiN<sub>x</sub>/PI and SiN<sub>x</sub>/PDMS/PI, using the lift-off technique illustrated in Fig. 1(a). The substrates for the SiN<sub>x</sub>/PI specimens were 25 μm thick Upilex-S (UBE Industries), while the substrates for the SiN<sub>x</sub>/PDMS/PI specimens were 70 μm thick Kapton-E (DuPont). Compared to Upilex-S, Kapton-E has a slightly lower Young's modulus but a slightly larger strain to failure. All the PI foils were ultrasonically cleaned with methanol and acetone, and then attached to a 3 mm thick Al plate using

double-sided tape. The bonded samples were pressed in a vacuum for 24 hours to remove bubbles between the PI foil and the Al plate.

The PDMS (Sylgard 184, Dow Corning) was prepared by mixing a silicone gel and a crosslinker in a 10:1 ratio by weight. A 10  $\mu\text{m}$  thick PDMS layer was then spin-coated on top of the Kapton-E. The specimens were degassed in a vacuum for 20 min, and cured for 1 hour at 80°C. The surface of the PDMS was made hydrophilic by treating it for 20 seconds with an O<sub>2</sub> plasma in a Technics Series 220 micro-stripper using a power of 75 W.

A 3.2  $\mu\text{m}$  thick positive photoresist (S1818, Microposit) was spin-coated on top of the Upilex-S and PDMS/Kapton-E. The coated samples were baked for 2 min at 115 °C and then exposed through a Cr mask using an MJB4 mask aligner (SUSS MicroTec). The samples were developed in MF-319 photoresist developer (Microposit), rinsed in DI water for 1 min, and dried with N<sub>2</sub> gas. The substrates were then cut into 7 mm  $\times$  60 mm rectangular strips and 500 nm SiN<sub>x</sub> films were deposited by chemical vapor deposition (CVD) in a NEXX system, with a base pressure of  $5 \times 10^{-6}$  Torr and a working pressure of 10 mTorr. The microwave power was 265 W and the substrate temperature was held at 22 °C. The gas flow rates for 3% SiH<sub>4</sub> (balance Ar), N<sub>2</sub>, and Ar were 40, 5.8, and 20 sccm respectively. Finally, the SiN<sub>x</sub> coatings were patterned by stripping the extra SiN<sub>x</sub> along with the remaining photoresist in acetone. At the same time, samples were detached from the Al plate. Islands of various sizes were used,  $L = 40 \mu\text{m}$ ,  $80 \mu\text{m}$ ,  $120 \mu\text{m}$ , or  $200 \mu\text{m}$ . The island thickness  $h = 500 \text{ nm}$  and the island period  $S/L = 1.5$  were the same for all specimens.

The specimens were stretched in a screw-driven tensile device (Figs.1b, c). A 5 mm  $\times$  5 mm square lattice of islands was placed at the center of the strip to make sure that they were subjected to uniform tensile strain. To reduce sliding between the specimens and the grips, two polymer tubes were attached to the samples with epoxy glue as shown schematically in Fig. 1(b). All tensile tests were performed in-situ under an optical microscope with CCD

camera. Applied strains were measured directly on the recorded micrographs.

Micrographs of the deformed islands are shown in Fig. 2. Islands on all SiN<sub>x</sub>/PI samples rupture at small strains. For samples with an island size of 200 μm, for instance, cracks first appear perpendicular to the tensile direction after an applied strain of 0.5%. As shown in Fig. 2(a), all islands are fractured at an elongation of 0.8%. If we reduce the island size, this strain-to-fracture increases slightly. For example, 40 μm SiN<sub>x</sub> islands start to crack when the substrate is stretched 0.9%. As shown in Fig. 2(b), all 40 μm islands have either cracked or debonded at an elongation of 2.1%.

By contrast, SiN<sub>x</sub>/PDMS/PI samples can be stretched to much larger strains. For samples with an island size of 200 μm, no crack or debond can be observed in any island after the sample is stretched by 20%, as shown in Fig. 2(c). Upon further stretching, islands start to wrinkle due to the compressive transverse strain. Eventually, cracks appear in the islands at an elongation of 24.7%, as shown in Fig. 2(d). Island rupture can be suppressed by decreasing the island size. It was impossible to fracture islands smaller than 200 μm because the PI substrates ruptured at elongations of about 30%. This pronounced effect of the PDMS interlayer is also shown in Fig. 3, which plots the accumulated fraction of cracked islands as a function of applied strain.

Using the commercial finite element code ABAQUS, we established a 3D model of a unit cell of the periodic island lattice. Schematics of the top and side views of the model are shown in Fig. 4. Because of symmetry, only one quarter of the unit cell was modeled, as represented by the shaded area in Fig. 4(a). We modeled the islands, the interlayer and the substrate as homogeneous, isotropic linear elastic materials with Young's moduli  $E_{\text{SiN}_x} = 200$  GPa,  $E_{\text{PDMS}} = 1$  MPa, and  $E_{\text{PI}} = 9.2$  GPa, as well as Poisson's ratios  $\nu = 0.3$  for SiN<sub>x</sub> and PI, and  $\nu = 0.48$  for PDMS<sup>14-16</sup>. A uniform displacement  $u_{\text{appl}}$  was applied to the substrates in the  $x_1$ -direction, i.e., the applied strain was given by  $\epsilon_{\text{appl}} = 2u_{\text{appl}} / S$ .

The maximum tensile strain in the island,  $\varepsilon_{\max}$ , occurs at the center of the island edge, as labeled in Fig. 4(a). Fig. 5 plots ratios of the maximum strain in the island to the applied strain  $\varepsilon_{\text{appl}}$  obtained from the simulations as a function of the island size. The maximum strain drops substantially when PDMS is introduced between the islands and the substrates. The simulations also show that the smaller islands experience smaller strains, but the effect is much more pronounced if the PDMS is introduced.

Assume that islands fracture when  $\varepsilon_{\max}$  reaches a critical value  $\varepsilon_c = 0.6\%$ . If we define the strain to failure,  $\varepsilon_r$ , as the applied strain at which 50% of the islands are cracked, then  $\varepsilon_c/\varepsilon_r$  can be plotted for the experiments and directly compared with the simulation results. For SiN<sub>x</sub>/PI specimens with various island sizes, the experimental and corresponding FEM results are of the same order of magnitude. Compared to SiN<sub>x</sub>/PI specimens, strains in islands on SiN<sub>x</sub>/PDMS/PI specimens are much lower, which confirms our previous claim that the high stretchability of SiN<sub>x</sub>/PDMS/PI specimens is due to the reduced strains in the islands. Admittedly, it is a highly simplified assumption that all islands crack whenever  $\varepsilon_{\max} = \varepsilon_c$  independent of island sizes or thicknesses. This simple criterion only provides the correct order of magnitude when the FEM simulations are compared with the experiments. We will perform a more careful analysis of crack nucleation taking flaw size distributions into consideration in a future paper.

The strain in the islands on the PDMS interlayer can also be calculated using a shear-lag model.<sup>17</sup> Our calculation gives that

$$\frac{\varepsilon_{\max}}{\varepsilon_{\text{appl}}} = 1 - \frac{1}{\cosh\left(\frac{L}{2\Lambda}\right)}, \quad (1)$$

where

$$\Lambda = \sqrt{\frac{E_{\text{SiN}} H h}{\mu_{\text{PDMS}}}}. \quad (2)$$

Here  $\mu$  is the shear modulus and  $H$  is the thickness of the interlayer. Equation (1) is plotted as the dashed curve in Fig. 5. The prediction of the shear-lag model agrees well with the finite element calculation. The length scale  $\Lambda$  measures the distance over which normal strain builds up in the islands. For the materials used in this study, its value is approximately 1720  $\mu\text{m}$ , i.e., one order of magnitude larger than the island size  $L$ . Consequently, the maximum strain in the islands is very small. Islands that are much larger than  $\Lambda$ , on the other hand, will experience significant strain when the substrate is stretched.

Finally, we also performed a 2D island/substrate debonding analysis using the same finite element method mentioned in an earlier work.<sup>18</sup> We found that the energy release rate for debonding, another important failure mode, is also reduced by orders of magnitude once a soft interlayer is applied.

In summary, when a thin layer of PDMS is introduced between the  $\text{SiN}_x$  islands and the polyimide substrate, the substrate can be stretched beyond 20% without causing the islands to crack or debond. The soft PDMS layer acts as a buffer, isolating the  $\text{SiN}_x$  islands from most of the applied strain in the polyimide substrate. This mechanism is confirmed by using finite element simulations and a shear-lag model. Furthermore, the shear-lag model introduces a length scale to measure the effect of isolation.

This work was supported by the National Science Foundation (NSF) under Grant CMS-0556169, and by the Materials Research Science and Engineering Center (MRSEC) at Harvard University. It was performed in part at the Center for Nanoscale Systems (CNS), a member of the National Nanotechnology Infrastructure Network (NNIN), which is supported by the National Science Foundation under NSF Award No. ECS-0335765. CNS is part of the Faculty of Arts and Sciences at Harvard University. J.-Y.S. and K.H.O. thank the support from the Korea Science and Engineering Foundation (KOSEF) granted by the Korea government (MOST, No.R11-2005-065).

## References

- <sup>1</sup> J. A. Rogers, Z. Bao, K. Baldwin, A. Dodabalapur, B. Crone, V. R. Raju, V. Kuck, H. Katz, K. Amundson, J. Ewing, and P. Drzaic, *Proc. Natl. Acad. Sci. U. S. A.* **98**, 4835 (2001).
- <sup>2</sup> E. Bonderover and S. Wagner, *IEEE Electron Device Lett.* **25**, 295 (2004).
- <sup>3</sup> C. J. Brabec, *Sol. Energy Mater. Sol. Cells* **83**, 273 (2004).
- <sup>4</sup> E. Abad, S. Zampolli, S. Marco, A. Scorzoni, B. Mazzolai, A. Juarros, D. Gómez, I. Elmi, G. C. Cardinali, J. M. Gómez, F. Palacio, M. Cicioni, A. Mondini, T. Becker, I. Sayhan, *Sens. Actuator B-Chem.* **127**, 2 (2007).
- <sup>5</sup> T. Someya, Y. Kato, T. Sekitani, S. Iba, Y. Noguchi, Y. Murase, H. Kawaguchi, and T. Sakurai, *Proc. Natl. Acad. Sci. U. S. A.* **102**, 12321 (2005).
- <sup>6</sup> H. C. Ko, M. P. Stoykovich, J. Song, V. Malyarchuk, W. M. Choi, C. -J. Yu, J. B. Geddes III, J. Xiao, S. Wang, Y. Huang, and J. A. Rogers, *Nature* **454**, 748 (2008).
- <sup>7</sup> S. P. Lacour, S. Wagner, R. J. Narayan, T. Li, Z. Suo, *J. Appl. Phys.* **100**, 014913 (2006).
- <sup>8</sup> P. I. Hsu, R. Bhattacharya, H. Gleskova, M. Huang, Z. Xi, Z. Suo, S. Wagner, and J. C. Sturm, *Appl. Phys. Lett.* **81**, 1723 (2002)
- <sup>9</sup> R. Bhattacharya, S. Wagner, Y. -J. Tung, J. R. Esler, and M. Hack, *Proc. IEEE* **93**, 1273 (2005).
- <sup>10</sup> D. -Y. Khang, H. Jiang, Y. Huang, J. A. Rogers, *Science* **311**, 208 (2006)
- <sup>11</sup> D. -H. Kim, J. -H. Ahn, W. M. Choi, H. -S. Kim, T. -H. Kim, J. Song, Y. Y. Huang, Z. Liu, C. Lu, J. A. Rogers, *Science* **320**, 507 (2008).
- <sup>12</sup> H. Gleskova, S. Wagner, and Z. Suo, *Appl. Phys. Lett.* **75**, 3011 (1999).
- <sup>13</sup> R. Bhattacharya, A. Salomon, and S. Wagner, *J. Electrochem. Soc.* **153**, G259 (2006).
- <sup>14</sup> O. Tabata, K. Kawahata, S. Sugiyama, and I. Igarashi, *Sensors and Actuators* **20**, 135 (1989).
- <sup>15</sup> S. H. Yoo, C. Cohen, C. -Y. Hui, *Polymer* **47**, 6226 (2006).
- <sup>16</sup> The data sheet of Upilex-S, UBE INDUSTRIES.LTD.
- <sup>17</sup> Z. C. Xia, J. W. Hutchinson, *J. Mech. Phys. Solids*, **48**, 1107 (2000).
- <sup>18</sup> N. Lu, J. Yoon, and Z. Suo, *Int. J. Mater. Res.* **98**, 717 (2007).

## Figure Captions

Fig. 1. (a) Fabrication process for two sets of polyimide-supported island arrays: SiN<sub>x</sub>/PI and SiN<sub>x</sub>/PDMS/PI. (b) Schematics of the in situ uniaxial tensile test. (c) A picture of our homemade screw-driven tensile tester.

Fig. 2. Samples stretched horizontally: (a) SiN<sub>x</sub>/PI,  $L = 200 \mu\text{m}$ ,  $\epsilon_{\text{appl}} = 0.8\%$ , all islands have channel cracks. (b) SiN<sub>x</sub>/PI,  $L = 40 \mu\text{m}$ ,  $\epsilon_{\text{appl}} = 2.1\%$ , most islands are cracked but a few are debonded. (c) SiN<sub>x</sub>/PDMS/PI,  $L = 200 \mu\text{m}$ ,  $\epsilon_{\text{appl}} = 19.6\%$ , all islands are intact. (d) SiN<sub>x</sub>/PDMS/PI,  $L = 200 \mu\text{m}$ ,  $\epsilon_{\text{appl}} = 24.7\%$ , islands are wrinkled and cracked.

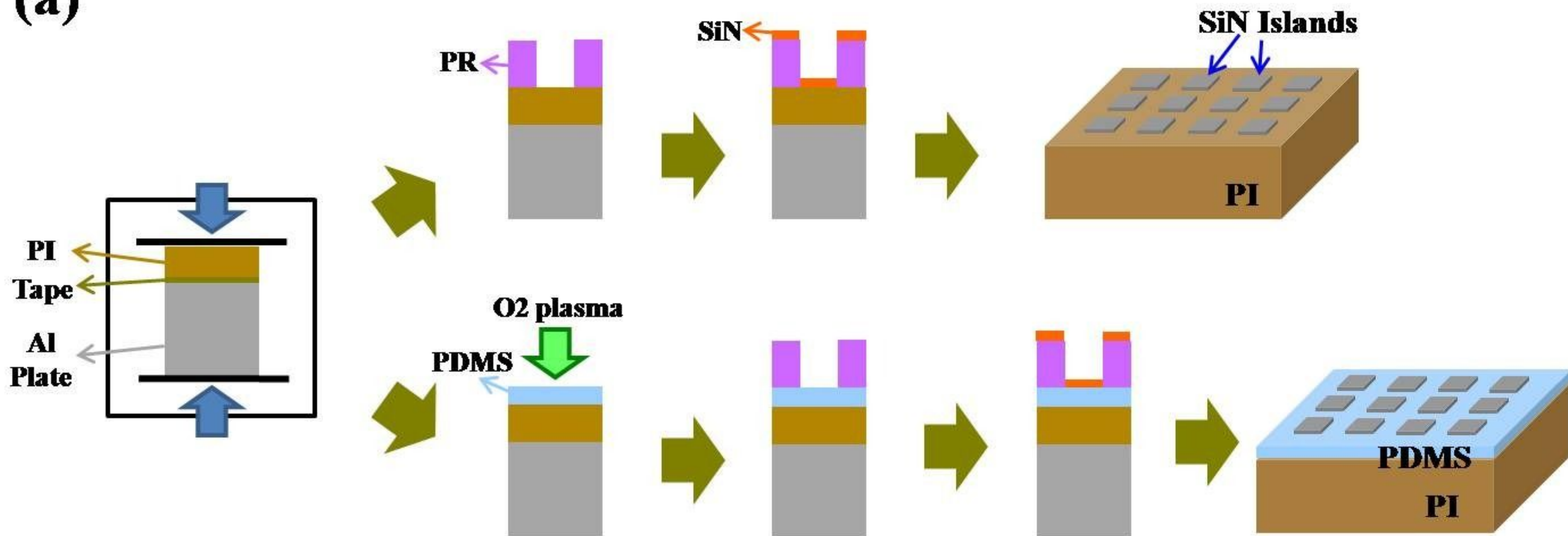
Fig. 3. The accumulated fraction of cracked islands is plotted as a function of the applied strain.

Fig. 4. Schematics of the 3D finite element model: (a) top view, (b) side view. (b) also depicts the 2D shear lag model.

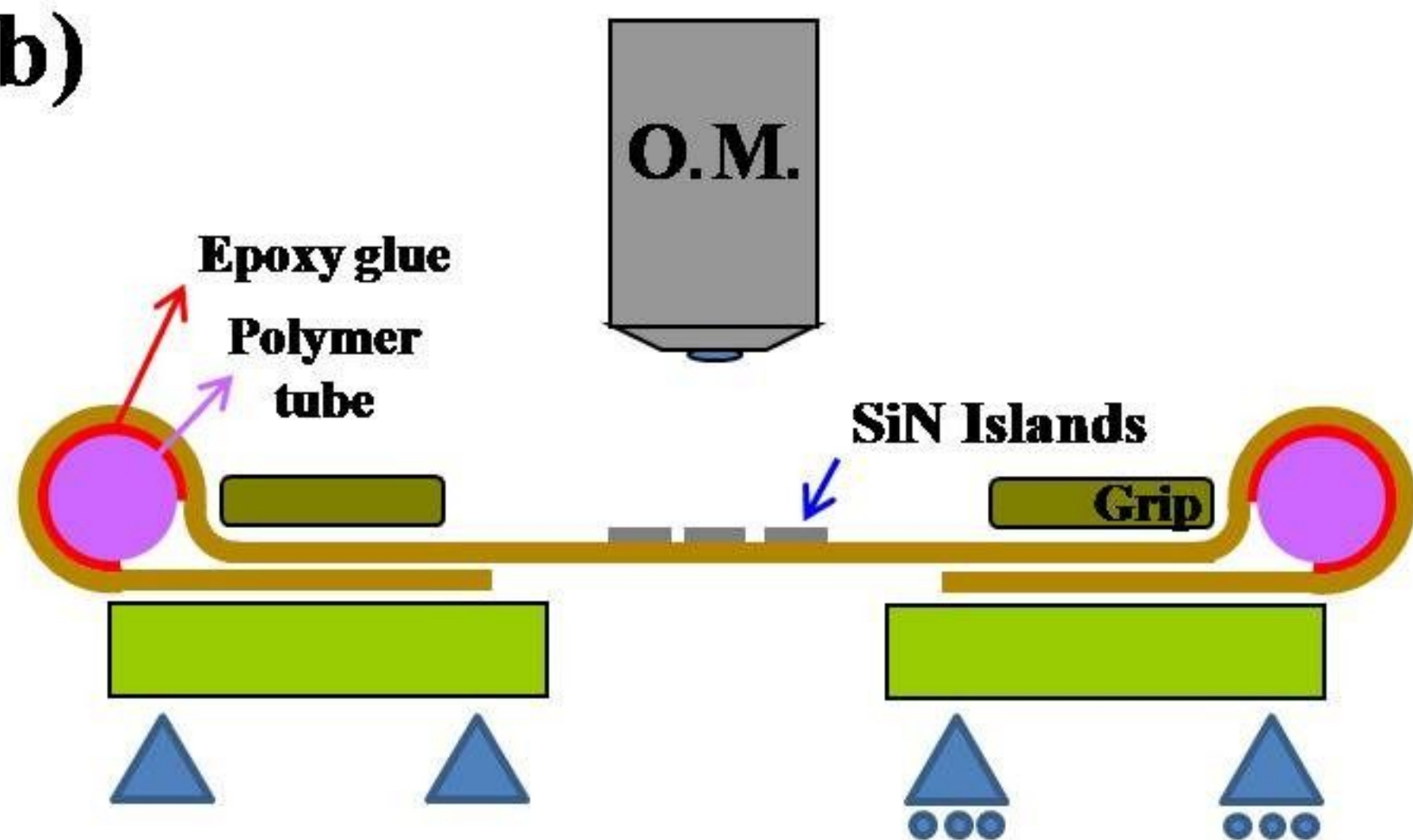
Fig. 5. Ratios of the maximum strain in the island to the applied strain obtained from 3D finite element simulations, experimental results, and calculations using a shear lag model. They all illustrate the fact that a soft interlayer can greatly reduce strains experienced by the islands.



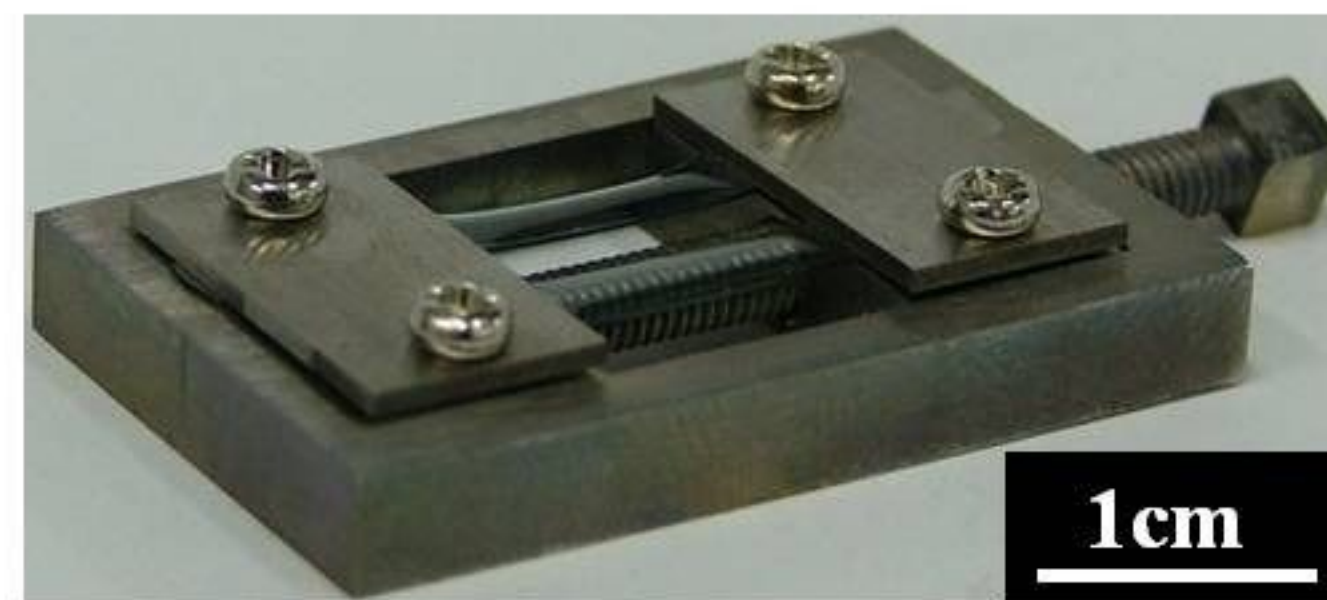
(a)

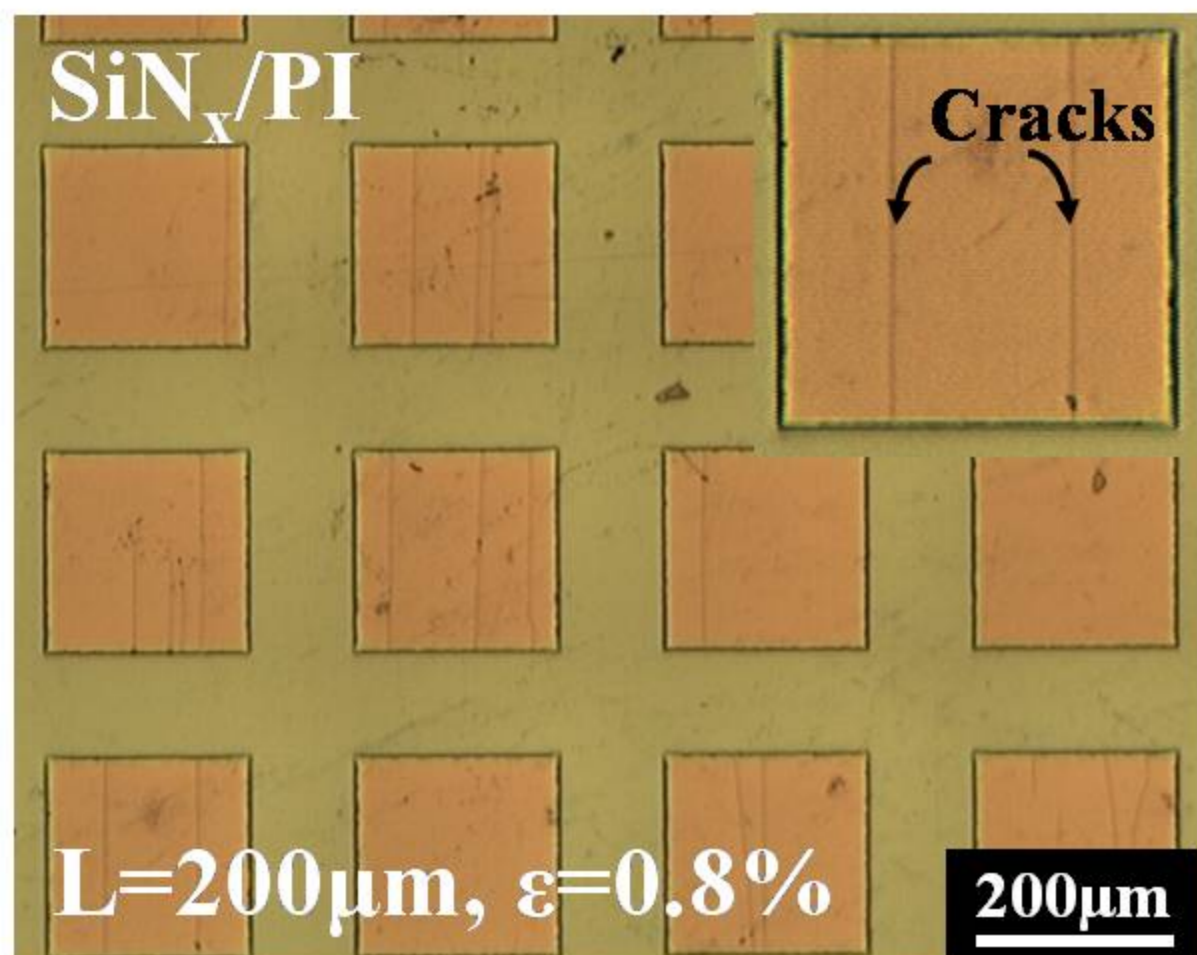
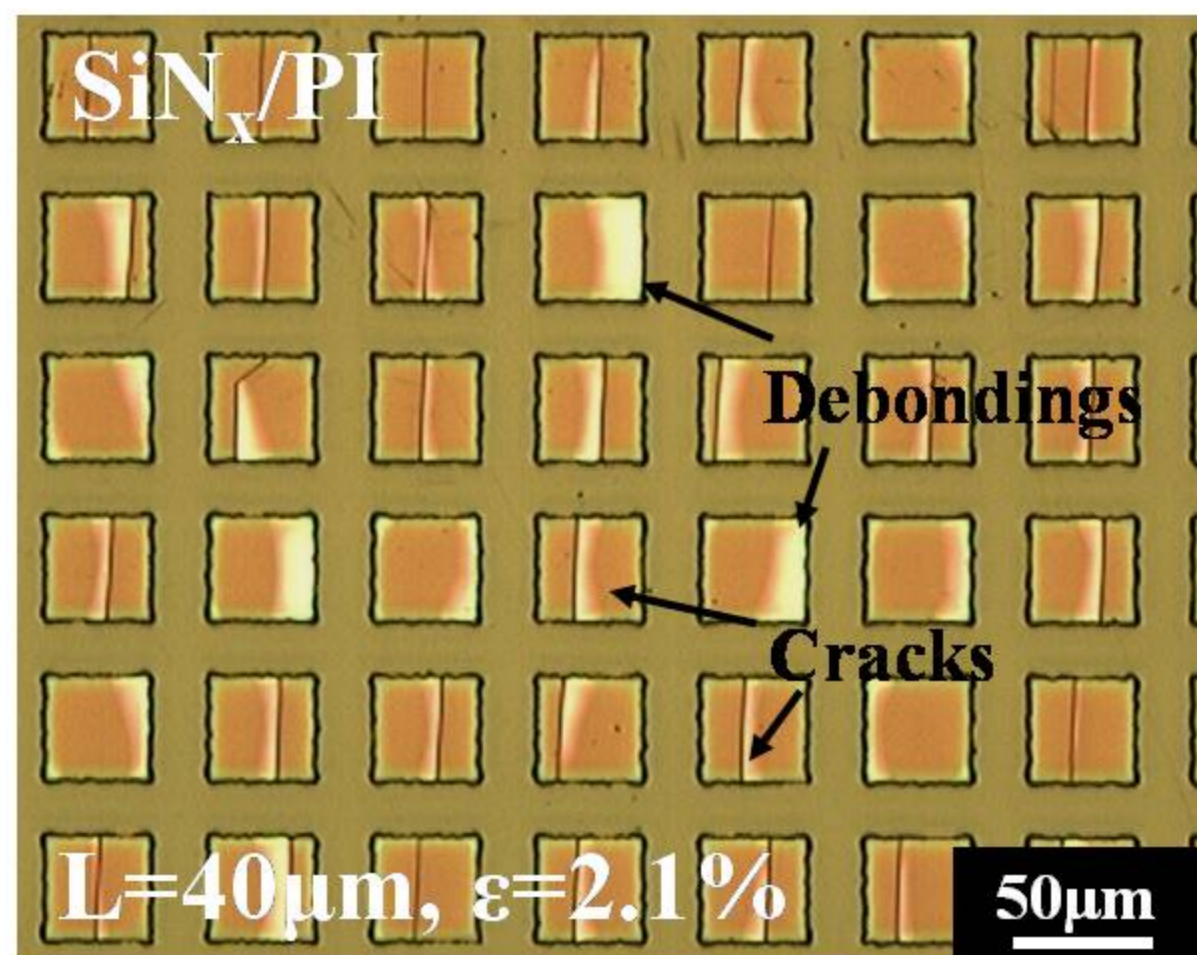
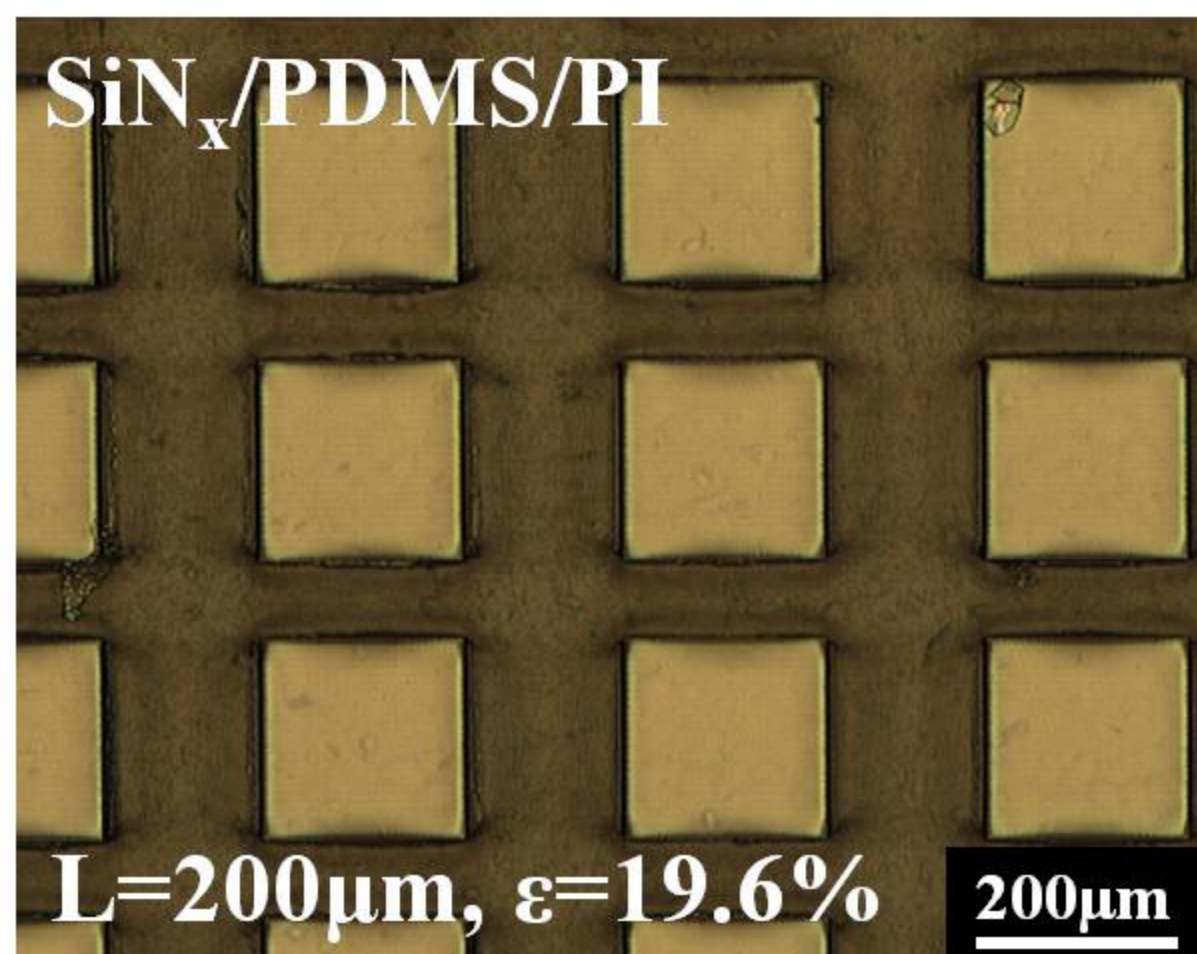
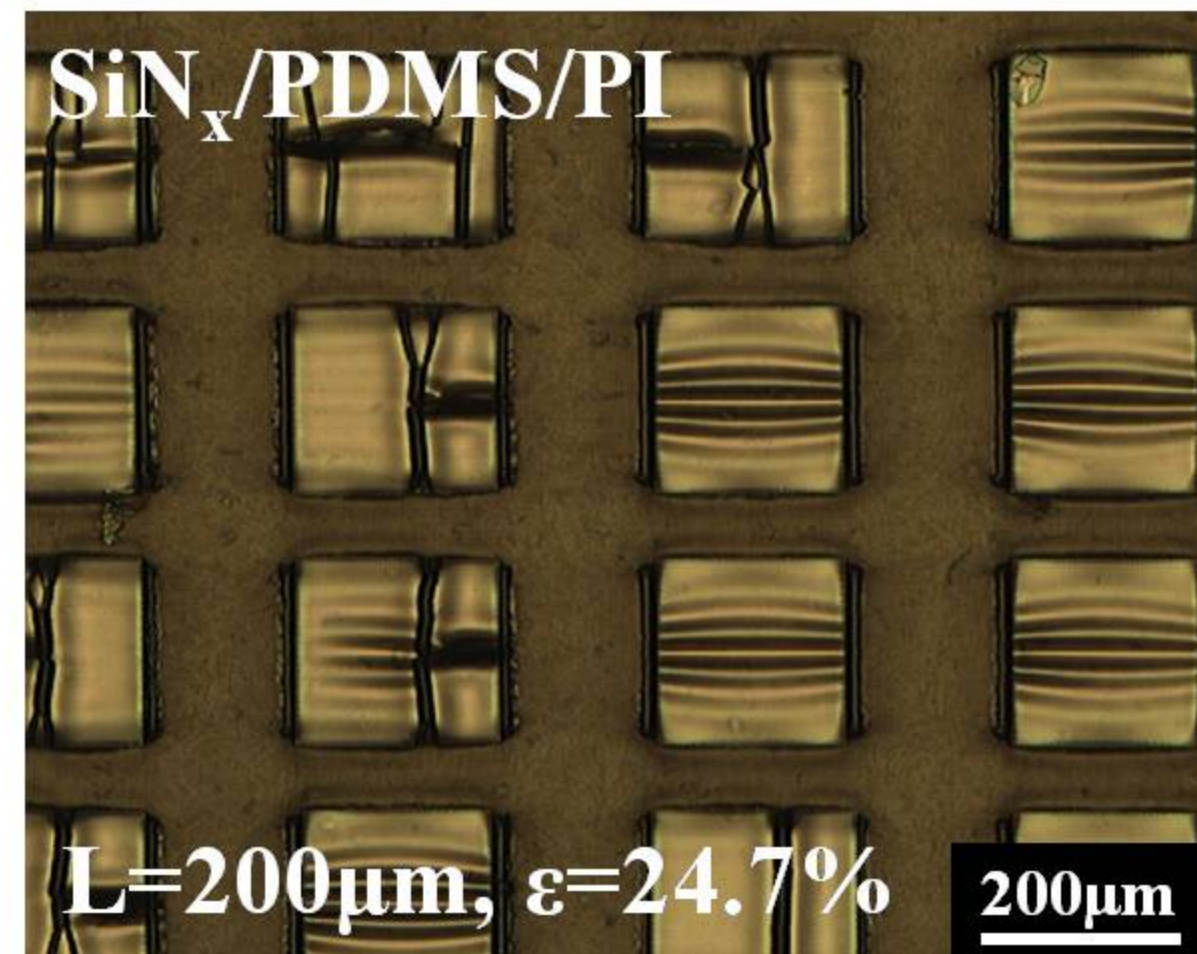


(b)

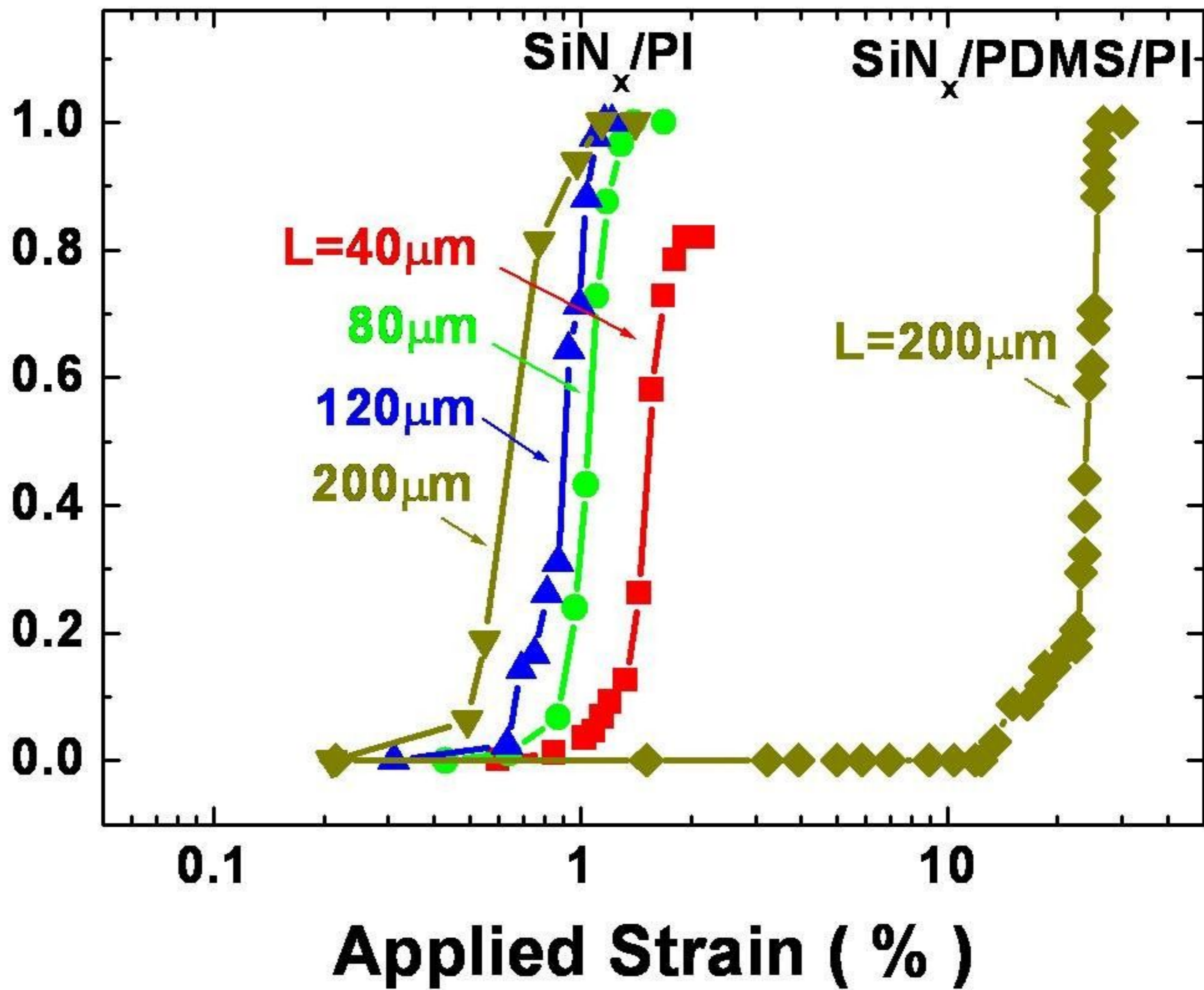


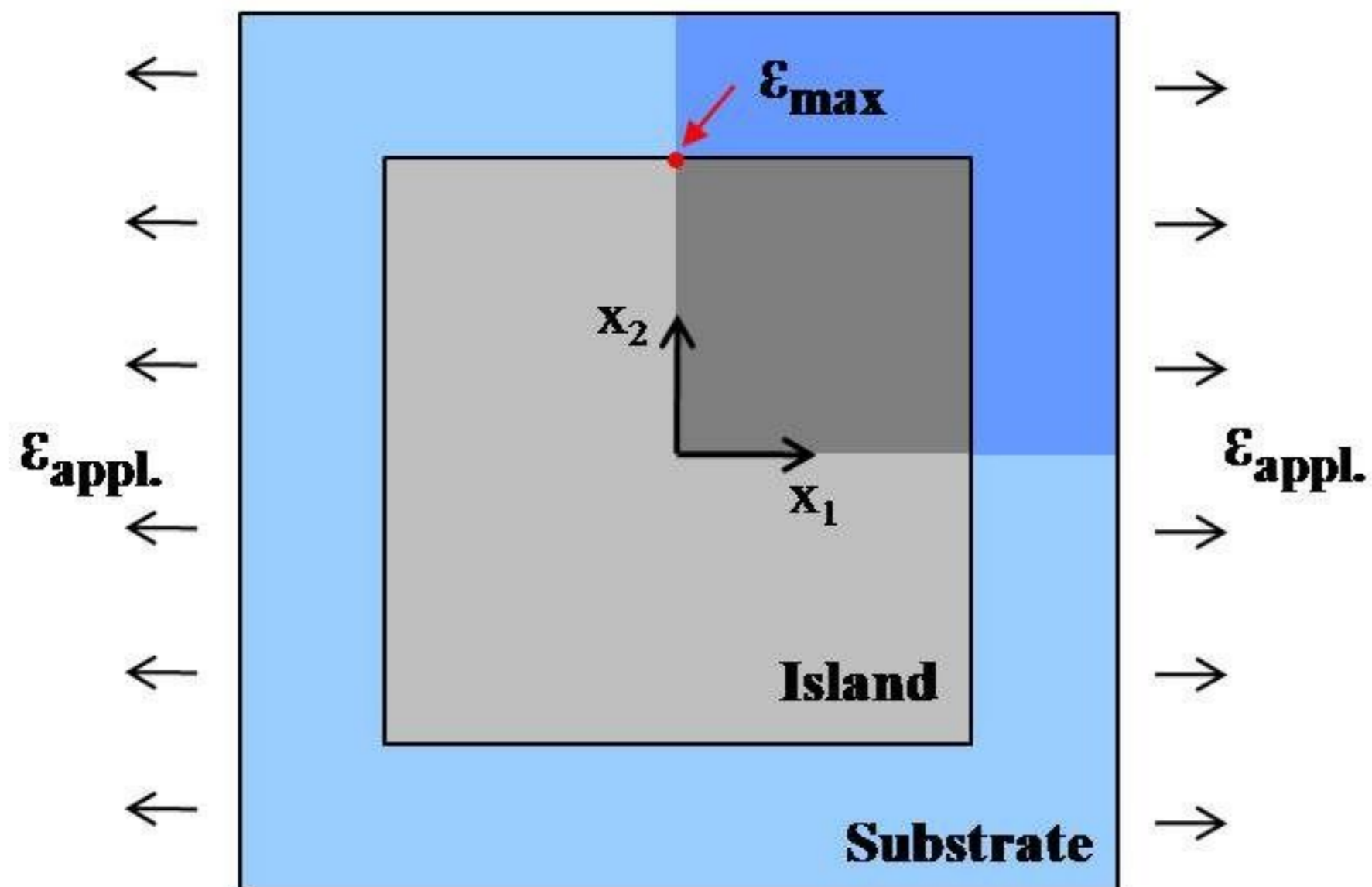
(c)



**(a)****(b)****(c)****(d)**

# Fraction of Cracked Islands



**(a)****(b)**